# A Differential SPDT T/R Switch for PMUT Biomedical Ultrasound Systems

Yaohua Zhang, Dai Jiang, and Andreas Demosthenous

Department of Electronic and Electrical Engineering, University College London, London WC1E 7JE, United Kingdom

yaohua.zhang@ucl.ac.uk; d.jiang@ucl.ac.uk; a.demosthenous@ucl.ac.uk

*Abstract*—This paper presents a differential T/R SPDT switch, designed in a 0.18 μm HV BCD technology for PMUT-based biomedical ultrasound systems. It incorporates a bootstrapping technique to pass high-voltage pulses and a shunt branch for improved isolation. The differential T/R switch is designed to interface with bimorph electrodes although a single-ended version can also interface with conventional PZT/CMUT transducers. Post-layout simulation results show that the switch circuit exhibits 64 Ω on-resistance and -62 dB off-isolation. A figure-of-merit is proposed to compare ultrasound T/R switches. To the best of the authors' knowledge, this differential switch is the first of its kind being reported for PMUT biomedical ultrasound systems.

*Keywords*—*CMOS integrated circuit, human-machine interface, PMUT, SPDT switch, T/R switch, ultrasound hand gesture recognition.*

## I. INTRODUCTION

Ultrasound is defined as sound with frequencies above 20 kHz and is beyond the human hearing range. In addition to the traditional applications of ultrasound in healthcare, recent research has successfully applied ultrasound in novel applications like fingerprint sensing [1], body fat measurement [2], and drone vision [3]. A new and emerging area of research is exploring the use of ultrasound in human-machine interfaces, more specifically wearable ultrasound hand gesture recognition as seen in Fig. 1(a) [4], [5]. The fundamental idea is to use ultrasound to detect morphological changes of both superficial and deep muscle fibres in the forearm as the user is conducting different hand gestures. After sufficient training, machine learning techniques would then be applied to decode the ultrasound signals to control a prosthetic hand. To this end, an ultrasound ASIC-based system architecture is proposed as shown in Fig. 1(b). It consists of four main parts: i) 8 ultrasound transducers distributed around the forearm in a wearable bracelet, ii) 8-channel ASIC with integrated analog front-end (AFE), analog-to-digital converter (ADC), power management unit (PMU), digital control unit (DCU) and iii) FPGA and PC for machine learning algorithms and prosthesis control.

Within the AFE, the transmit/receive (T/R) switch is a crucial interface circuit between the transducer and the transmit (TX) mode/receive (RX) mode circuits [6]. In TX mode, the T/R switch passes high-voltage pulses to the transducers while isolating the RX circuits from the high-voltage pulses. This isolation is necessary because RX circuits are typically constructed from low-voltage transistors that can be damaged by the high-voltage (HV) pulses used to drive the transducers. In RX mode, the T/R switch is configured as a low on-resistance ($R_{on}$) switch to pass the received signals
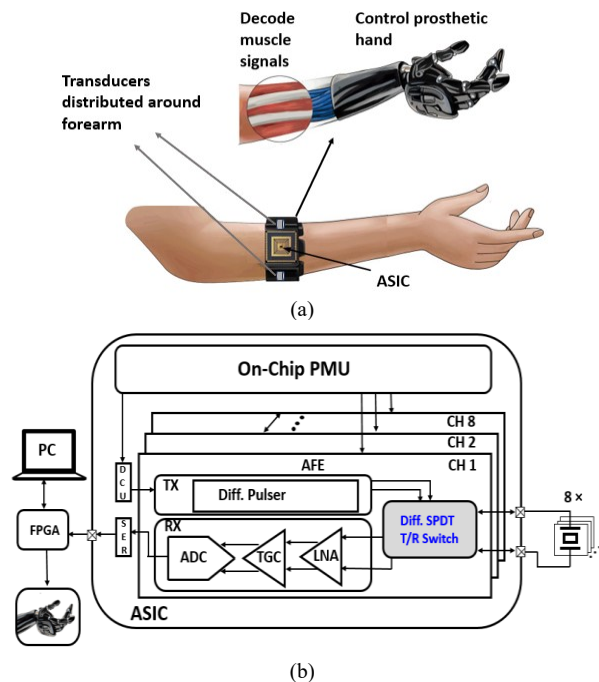
Fig. 1. (a) Artist impression of the wearable ultrasound hand gesture recognition concept. (b) Proposed architecture of the ultrasound hand gesture recognition system.

with minimal attenuation and distortion from the transducers to the subsequent RX circuits.

The design of a T/R switch depends on the type of transducers. By virtue of their construction, piezoelectric transducers (PZTs) and capacitive micromachined ultrasonic transducers (CMUTs) are typically modelled as single-ended sources. T/R switches and the subsequent RX circuits designed for PZT or CMUT systems are generally single-ended. On the other hand, piezoelectric micromachined ultrasonic transducers (PMUTs) are a relatively new type of transducer and area game changer in ultrasound system research. From a circuit design perspective, an important advantage that PMUTs offer is that they allow for fully differential circuits. Due to its physical structure, a PMUT, more specifically bimorph PMUT can act as a *differential* load (TX mode) or *differential* source (RX mode). Therefore, with bimorph PMUTs, both the TX and RX circuits can be designed to be fully differential and reap well-known benefits including reduced crosstalk and higher linearity. When interfacing with PMUTs (differential source), a single-ended single-pole single-throw (SPST) T/R switch typically used in PZT/CMUT-based applications is not the most suitable option. PMUT-based ultrasound systems demand a more appropriate T/R switch solution.

This paper is focused on the design of a differential single-pole double-throw (SPDT) T/R switch as part of an ASIC in wearable ultrasound hand gesture recognition system (Fig. 1(b)). The proposed switch is also applicable to other ultrasound systems that support differential interfacing to the transducers. The rest of the paper is organised as follows. Section II elaborates on the bimorph PMUT as a differential source, Section III discusses the proposed switch circuit, Section IV presents post-layout simulation results and Section V concludes the paper.

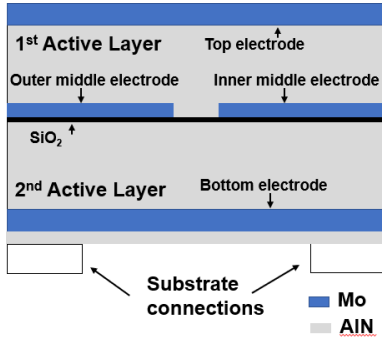## II. BIMORPH PIEZOELECTRIC MICROMACHINED ULTRASONIC TRANSDUCER
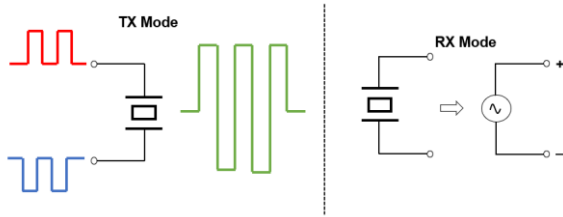


Fig. 2. Bimorph PMUT structure [7].



Fig. 3. Operation of the bimorph PMUT in TX and RX modes.

A PMUT is a microelectromechanical systems (MEMS) device, in which microscopic-scale resonators are grown on a silicon wafer, making PMUTs CMOS-friendly. Recently, bimorph PMUTs have been proposed [8], [9] and its structure is shown in Fig. 2. A bimorph PMUT is made from an AlN/Mo/AlN stack and consists of four electrodes, namely the top and bottom electrodes which can be grounded as well as the inner middle and outer middle electrodes that act as two active electrodes. In TX mode, the bimorph PMUT can be driven differentially by pulsers as shown in Fig. 3, whereas in RX mode the bimorph PMUT acts as a differential signal source. The term "bimorph" emphasises the fact that there are *two* active electrodes in contrast to unimorphs that only have one active electrode such as PZTs and CMUTs. Bimorph PMUTs have been experimentally verified to exhibit higher drive sensitivity and electromechanical energy efficiency than unimorph PMUTs [8], making bimorph PMUTs an excellent candidate for ultrasound systems. Note that in some PMUT-based ultrasound systems, one electrode is grounded, thus these PMUTs can only support single-ended operation [10], [11]. In this paper, PMUTs refer to bimorph structures that support differential operation.
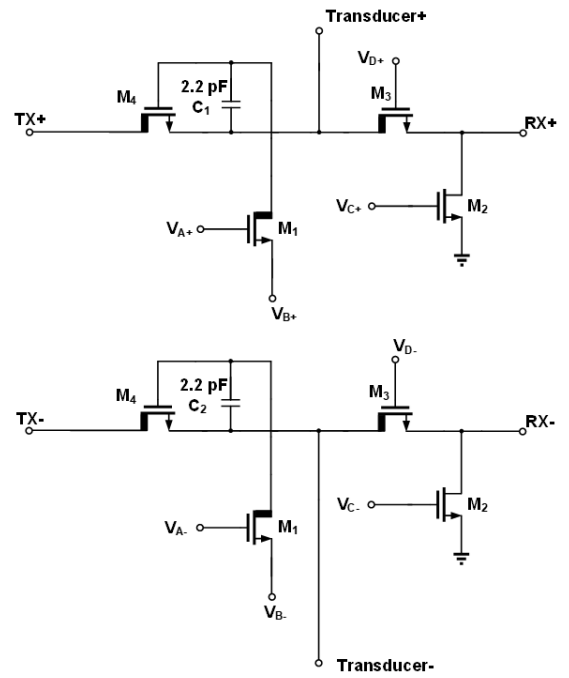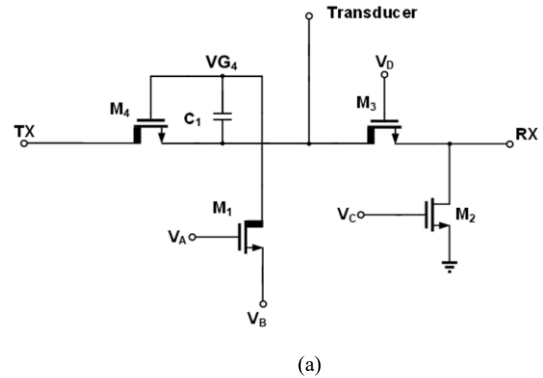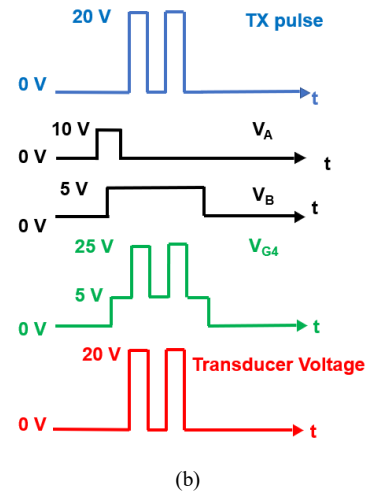


Fig. 4. Proposed differential switch. Thick drain devices indicate LDMOS, whereas standard NMOS symbols refer to a 3.3 V low-voltage transistor.



(a)



(b)

Fig. 5. (a) Single-ended half-circuit. (b) Control waveforms.

## III. PROPOSED SWITCH CIRCUIT

The differential SPDT switch in Fig. 4 was designed to interface with bimorph PMUTs. There are several recently published designs that use two single-ended SPST switches to

interface with differential bimorph PMUTs [3], [7]. In these designs, the pulsers are directly connected to the PMUTs, leaving the SPST switches connected to the inputs of the LNAs instead. Although this is valid, the use of SPST switches is not a flexible solution because these switches can only be used for isolation, but they cannot be configured to pass high-voltage pulses to the transducers when required. For instance, in area-constrained applications, it is very area-expensive to integrate pulsers on-chip. As a workaround, HV pulses are generated off-chip and HV switches are used to transfer the HV pulses to the transducers [12]. A differential SPDT T/R switch that can isolate the RX circuits while passing high-voltage pulses to the transducers in TX mode as well as passing received signals from the transducer to the RX circuits in RX mode would be a more versatile solution from a system-level perspective.

The operation of the differential SPDT switch can be best explained by considering its half-circuit as shown in Fig. 5(a). In RX mode, the series transistor $M_3$ is turned on, shunt transistor $M_2$ is turned off and the TX side disabled. The switch should have a low $R_{on}$. A low $R_{on}$ is beneficial for reducing thermal noise and will not degrade the signal-to-noise ratio of the RX circuits. The designer typically needs to increase the size of the transistor $M_3$ and/or raise its $V_{GS}$ to achieve low $R_{on}$. However, raising the $V_{GS}$ is a rather limited strategy because the maximum $V_{GS}$ of a LDMOS is normally quite low when compared to the maximum $V_{DS}$ that the LDMOS can withstand. The LDMOS used in this design can accommodate a maximum $V_{DS}$ and $V_{GS}$ of 45 V and 18 V respectively. On the other hand, by increasing the size of the transistor $M_3$, the transistor will exhibit greater parasitic capacitances, which will worsen the off-isolation due to signal leakage through these parasitic capacitances. To improve off-isolation, a shunt transistor $M_2$ is included to provide a low-impedance path to ground.

In the TX mode, $M_3$ is turned off and $M_2$ is turned on to isolate the RX circuit from HV pulses. The TX switch is designed as an area-efficient bootstrapped switch, adapted from [12]. In contrast to that in [12], the proposed switch is more area-efficient as it removes the redundant diodes to consist of only two LDMOS ($M_1$, $M_4$) and one capacitor ($C_1$). Unlike [12], the proposed switch does not require forward biased diodes to operate. Note that in most p-substrate CMOS technologies, a forward biased pn junction is either forbidden or discouraged as it requires additional processes to guarantee that substrate leakage current does not damage the die.

The TX side is designed to transfer a 0 V to 20 V, 1 MHz square pulse to the transducer (modelled as a 20-pF load). To do so, $M_4$ is turned on and the high-voltage pulses pass from its drain to its source, which is also connected to the transducers. Comprehensive simulations showed that a $V_{GS4}$ of around 5 V is required to turn on $M_4$ to an acceptable $R_{on}$. Hence, the $V_{G4}$ is required to be as high as 25 V when passing the 20 V pulses to the transducers. With a $V_{GS}$ limit of 18 V, this implies that a simple 0 V (low) / 25 V (high) signal cannot be used to control $V_{G4}$. Instead, a bootstrapped switch has been designed that ensures a 5 V offset between the gate and source of $M_4$ even when passing the 20 V pulses. As seen from Fig. 5(b), when $V_A$ and $V_B$ are both high, $V_{GS1}$ is equal to 5 V, turning $M_1$ on and charging the top plate of $C_1$ ($V_{G4}$) to 5 V which also turns $M_4$ on. When the high-voltage pulses arrive, $M_{G4}$ is bootstrapped and $C_1$ maintains the required overdrive voltage to keep $M_4$ on.
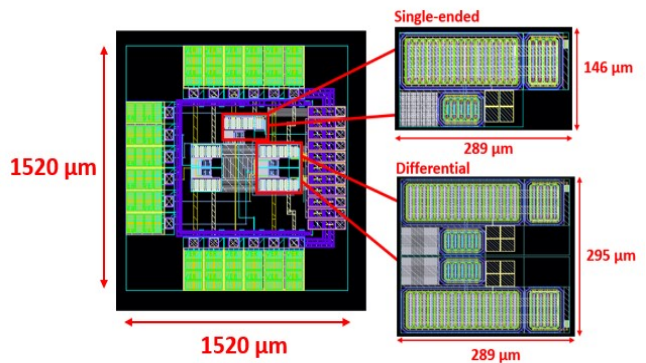


Fig. 6. Complete chip-level layout, with zoomed-in views of the single-ended and differential switches. Unlabeled blocks are test structures.
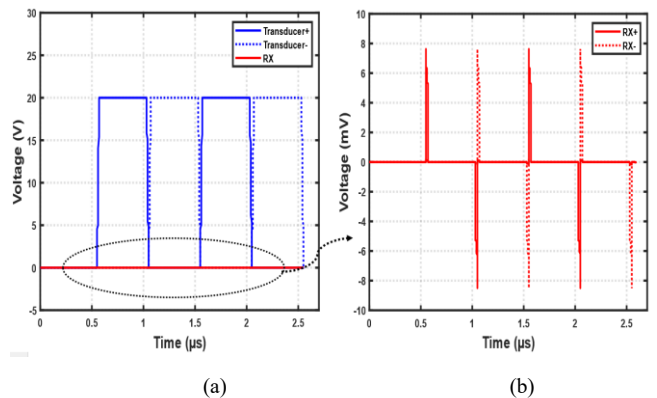


(a)                                      (b)

Fig. 7. (a) Differential TX mode switch waveforms. 20 Vpp, 1 MHz square pulses seen at the transducers. (b) Very small voltage spikes at RX circuit input (zoomed-in view), indicating good off-isolation.
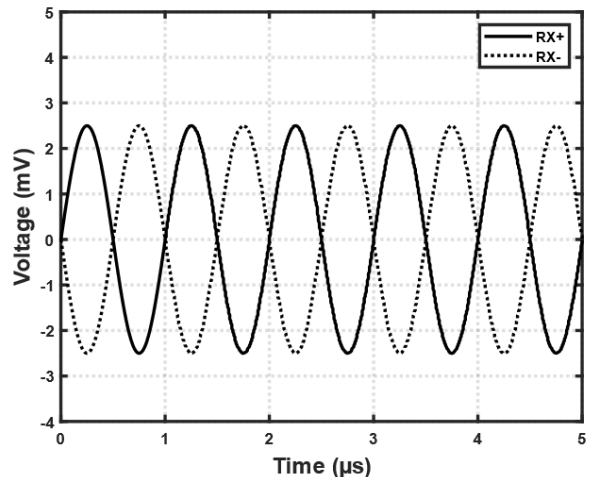


Fig. 8. Differential RX mode switch output waveforms.

## IV. POST-LAYOUT SIMULATION RESULTS

The circuit was developed in a 0.18 μm HV BCD technology. It was carefully designed and optimised for the conflicting objectives of low $R_{on}$, high off-isolation and acceptable area. The complete chip-level layout is shown in Fig. 6. The circuit occupies 289 μm × 146 μm and 289 μm × 295 μm for the single-ended half-circuit and differential circuit respectively. The differential circuit was carefully laid out to be as symmetrical and balanced as possible.

| | This work (post-layout simulation) | [13] | [14] | [15] |
|---|---|---|---|---|
| Technology | **0.18 µm HV BCD** | 0.18 µm HV SOI | 0.35 µm HV CMOS | 0.7 µm HV BCD |
| $R_{on}$ (Ω) | **64** | 290 | 180 | 200 |
| $ISO_{off}$ (dB) | **-62** | -64 | -17.52 | -30 |
| FoM | **0.97** | 0.22 | 0.097 | 0.15 |
| Area/ch (µm²) | **42190[a], 85260[b]** | 9920 | 48320 | 920000[c] |
| Number of HV MOS/channel | **3[a], 6[b]** | 3 | ≥ 5 | ≥ 4 |
| Single-ended/differential | **Both** | Single-ended | Single-ended | Single-ended |

[a]Single-ended. [b]Differential. [c]Estimated from paper.

The differential operation of the switch in the TX mode is shown in Fig. 7(a). It shows the differential 20 V transmitted pulses being delivered to the transducers (modelled as 20 pF load) while the RX circuit side is successfully isolated, exhibiting only small voltage spikes (Fig. 7(b)).

The differential operation of the switch in RX mode is shown in Fig. 8. The T/R switch output signals are transferred with minimal attenuation and distortion when given differential 1 MHz, 5 $mV_{p-p}$ sinusoidal input signals (mimicking received ultrasound signals).

Table I summarises the performance of the proposed circuit and compares it to the state-of-the-art. The area comparison is rather subjective and arbitrary because the occupied area is directly influenced by the chosen technology. Older process nodes and technologies that use junction isolation for high-voltage isolation (this work) tend to occupy bigger area than high-voltage SOI technology used in [13]. Furthermore, it is inevitable for a differential design to take up more area than a single-ended design. A fairer comparison would compare the number of high-voltage transistors used in the design as a proxy for area. It can be seen from Table I that the proposed circuit is comparable to the state-of-the-art in this regard.

The two most important specifications for a T/R switch in ultrasound applications are its $R_{on}$ and off-isolation ($ISO_{off}$). These two specifications are integral to the function of the switch, and it is logical to construct a figure-of-merit (FoM) from these two specifications. In this paper, a simple but insightful FoM to compare ultrasound T/R switches is proposed and given by (1).

$$FoM = |ISO_{off}(dB)| / R_{on} (\Omega). \qquad (1)$$

Since the T/R switch should have large off-isolation and low $R_{on}$ ideally, a higher FoM is desirable. The proposed switch achieves an FoM of 0.97, which is a 4.4 × improvement over the latest published work [13].

## V. Conclusion

A differential SPDT switch for PMUT-based applications has been presented. Its single-ended half-circuit version is also equally applicable to PZT/CMUT (unimorph) applications. The switch has been designed in a 0.18 µm HV BCD technology. A new FoM used to compare ultrasound T/R switches is also proposed. The performance of the proposed switch achieves a 4.4 × improvement over the state-of-the-art. To the best of the authors' knowledge, the proposed differential switch is the first of its kind.

## References

[1] H. -Y. Tang et al., "3-D ultrasonic fingerprint sensor-on-a-chip," *IEEE J. Solid-State Circuits*, vol. 51, no. 11, pp. 2522-2533, Nov. 2016.

[2] H. -Y. Tang, Y. Lu, S. Fung, D. A. Horsley and B. E. Boser, "11.8 Integrated ultrasonic system for measuring body-fat composition," *IEEE Int. Solid-State Circuits Conf. (ISSCC) Dig. Tech. Papers*, Feb. 2015, pp. 1-3.

[3] L. Wu et al., "An ultrasound imaging system with on-chip per-voxel RX beamfocusing for real-time drone applications," *IEEE J. Solid-State Circuits*, vol. 57, no. 11, pp. 3186-3199, Nov. 2022.

[4] Y. Zhang et al., "A four-channel analog front-end ASIC for wearable a-mode ultrasound hand kinematic tracking applications," in *Proc. IEEE Biomed. Circuits Syst. Conf.*, pp. 1-4, 2023.

[5] X. Yang et al., "Simultaneous prediction of wrist and hand motions via wearable ultrasound sensing for natural control of hand prostheses," *IEEE Trans. Neural Syst. Rehabil. Eng.*, vol. 30, pp. 2517-2527, Aug. 2022.

[6] Y. Zhang and A. Demosthenous, "Integrated circuits for medical ultrasound applications: imaging and beyond," *IEEE Trans. Biomed. Circuits Syst.*, vol. 15, no. 5, pp. 838-858, Oct. 2021.

[7] J. Lee et al., "A 36-channel auto-calibrated front-end ASIC for a pMUT-based miniaturized 3-D ultrasound system" *IEEE J. Solid-State Circuits*, vol. 56, no. 6, pp. 1910-1923, Jun. 2021.

[8] S. Akhbari, F. Sammoura, B. Eovino, C. Yang and L. Lin, "Bimorph piezoelectric micromachined ultrasonic transducers," *J. Microelectromech. Syst.*, vol. 25, no. 2, pp. 326-336, Apr. 2016.

[9] Z. Shao, S. Pala, Y. Peng and L. Lin, "Bimorph pinned piezoelectric micromachined ultrasonic transducers for space imaging applications," *J. Microelectromech. Syst.*, vol. 30, no. 4, pp. 650-658, Aug. 2021.

[10] L. Novaresi et al., "A PMUT transceiver front-end with 100-V TX driver and low-noise voltage amplifier in BCD-SOI technology," in *Proc. IEEE 48th Eur. Solid State Circuits Conf.*, 2022, pp. 221-224.

[11] I. Zamora, E. Ledesma, A. Uranga and N. Barniol, "Phased array based on AlScN piezoelectric micromachined ultrasound transducers monolithically integrated on CMOS," *IEEE Electron Device Lett.*, vol. 43, no. 7, pp. 1113-1116, Jul. 2022.

[12] M. Tan et al., "A front-end ASIC with high-voltage transmit switching and receive digitization for 3-D forward-looking intravascular ultrasound imaging," *IEEE J. Solid-State Circuits*, vol. 53, no. 8, pp. 2284-2297, Aug. 2018.

[13] S. Kajiyama et al., "T/R switch composed of three HV-MOSFETs with 12.1-µW consumption that enables per-channel self-loopback AC tests and −18.1-dB switching noise suppression for 3-D ultrasound imaging with 3072-ch transceiver," *IEEE Trans. Very Large Scale Integr. (VLSI) Syst.*, vol. 30, no. 2, pp. 153-165, Feb. 2022.

[14] H. Jung et al., "CMOS high-voltage analog 1–64 multiplexer/demultiplexer for integrated ultrasound guided breast needle biopsy," *IEEE Trans. Ultrason., Ferroelect., Freq. Control*, vol. 65, no. 8, pp. 1334-1345, Aug. 2018.

[15] Y. Li, R. Wodnicki, N. Chandra and N. Rao, "An integrated 90V switch array for medical ultrasound applications," in *Proc. IEEE Custom Integr. Circuits Conf.* 2006, 2006, pp. 269-272